Main Menu

- Home
- Welcome
- Introductory Matters
- Program at a Glance
- Sessions
- Author Index
- Digest Book
- Instructions for use

WELCOME TO INTERMAG EUROPE 2008 CD

The INTERMAG Europe 2008 Conference is to be held in the *Palacio Municipal de Congresos de Madrid*, from **May 4 to May 8, 2008**.

Information related to the location, conference registration, publications, presentations, posters, etc can be found in the introductory sections of the Advance Program Book. For more information please check the conference web-site at http://www.intermagconference.com/intermag2008.

To view the digests of the papers to be presented at the conference you will need to have Adobe Acrobat Reader installed on your computer. If you do not have this available Click here to install the software on your laptop.

GP-04. **Comparison of iron losses in switched reluctance motor with different winding arrangements and switching sequences.** *T. Sun*[1] and J. Hong[1] *1. Department of Mechanical Engineering, Hanyang University, Seoul, South Korea*

GP-05. **Optimum Design Criteria for Maximum Torque Density and Minimum Torque Ripple of Synchronous Reluctance Motor according to the Rated Wattage using Response Surface Methodology.** *Y. Choi*[1] and S. Mun[1] *1. Electrical Eng., Hanbat National University, Deajeon, South Korea*

GP-06. **The Evaluation of On-line Observer System of Synchronous Reluctance Motor Using a Coupled FEM & Preisach Model.** *H. Lim*[1], J. Lee[1], M. Lee[1] and D. Lee[2] *1. Electrical Engineering, Hanbat National University, Daejeon, South Korea; 2. Electrical Engineering, Hanyang University, Seoul, South Korea*

GP-07. **Design and Characteristic Analysis of Synchronous Reluctance Motors with Axial Lamination Rotor.** *S. Hahn*[1], J. Hong[1], J. Kim[1] and D. Koo[2] *1. Department of Electrical Engineering, Dong-A University, Busan, South Korea; 2. Mechatronics Research Group, Korea Electrotechnology Research Institute, Changwon, South Korea*

GP-08. **Design Solutions To Minimize Iron Core Loss In Synchronous Reluctance Motors Using Preisach Model & Finite Elements Method(FEM).** *H. Lim*[1], J. Lee[1], M. Lee[1] and D. Lee[2] *1. Hanbat National University, Daejeon, South Korea; 2. Electrical Engineering, Hanyang University, Seoul, South Korea*

Comparison of Iron Losses in Switched Reluctance Motor with Different Winding Arrangements and Switching Sequences

Tao Sun[1], Ji-Young Lee[2], and Jung-Pyo Hong[1], *Senior Member, IEEE*

[1]School of Mechanical Engineering, Hanyang University, Seoul, CO 133791, Korea
[2]Korea Electrotechnology Research Institute, Changwon, CO 641120, Korea

This paper presents a comparison of iron losses for switched reluctance motors (SRM) considering four different winding arrangements and/or switching sequences. These four cases are the concentrated winding with unipolar switching sequence, the concentrated winding with bipolar switching sequence, the distributed winding with bipolar switching sequence, and the toroidal winding with bipolar switching sequence, respectively. A series of numerical method which is composed of the magneto-static field finite element analysis, Fourier transform and experimental iron-loss curves is used to evaluate the iron losses of each model. Finally, the iron losses in the stator and rotor, and the ratio of the total iron losses to the input power will be compared. These results can give more reference for the SRM design and the drive selection.

***Index Terms*—FEA, Iron Losses, Switched Reluctance Motor, Winding Arrangement**

I. Introduction

SWITCHED RELUCTANCE MOTORS (SRM) have been applied in many fields such as industry, home appliances and vehicles due to the low-cost manufacture, and simple and strong structure. However, some drawbacks including low electrical utilization, acoustic noise and special drive much limit the performance and application. In order to improve these shortages, except the optimal structure design, several different stator winding arrangements and switching sequences also have been proposed [1]-[4].

Although all these improvement methods claimed that the advantages in dynamic performance were achieved, none of them demonstrated the steady-state characteristics, especially in the aspect of losses and efficiency. When the structure, dimension, and number of turns are the same, the copper losses and mechanical losses become identical, i.e., the efficiency and losses is represented by iron losses. As well known, the iron losses consist of hysteresis loss and eddy-current loss [5]-[7]. The hysteresis loss is proportional to the frequency and amplitude of flux density, while the eddy-current loss is proportional to the square of the both. Thus, the different winding arrangements and switching sequences may directly cause different magnetic flux distribution and lead that the frequency and amplitude of flux density change with it.

This paper will compare the iron losses of SRMs with different winding arrangements and switching sequences by using magneto-static field finite element analysis (FEA) and numerical iron losses calculation method. The ideal rectangular driving current and hence non-sinusoidal flux densities make the conventional iron-loss calculation method unavailable. This paper adopts the method which was introduced and verified in [7] to solve this problem. By using of the Discrete Fourier Transform (DFT) and experimental iron-loss data curves, this method can evaluate iron losses with any shape and period of flux density. Finally, the iron losses in the stator and rotor, and the ratio of the total iron losses to the input power will be compared. These results can give more reference for the SRM design and the selection of drive method.

II. Analyzed SRM Models

The fundamental structure of the analyzed SRM model is a typical 6-slot/4-pole V-type. The common dimensions are shown in Table I. The conventional concentrated winding, distributed winding and toroidal winding are combined with this structure and named CSRM, DSRM, and TSRM for short, respectively. The different winding arrangement requires the corresponding switching sequence to drive. Specially, for the concentrated winding arrangement, an additional bipolar switching sequence is adopted and named CSRM2 to distinguish the unipolar drive (CSRM1). The motor models with winding arrangement and corresponding switching sequence are shown in Fig. 1.

TABLE I
DIMENSION OF ANALYZED SRM

Parameter	Value	
Stator outer diameter	140	mm
Rotor outer diameter	71.6	mm
Rotor stack length	97	mm
Air gap length	0.3	mm
Stator pole arc/Rotor pole arc	30/31	°
Turns per pole	60	-

III. Iron Loss Calculation Method

The general expression of iron losses which includes the hysteresis loss $P_{h,}$ eddy current loss P_e and a anomalous component P_a is shown in (1) [5]-[6].

$$P_c = P_h + P_e + P_a = k_h f B_m^{\alpha} + k_e f^2 B_m^2 + k_a f^{1.5} B^{1.5} \qquad (1)$$

where the coefficients k_h, k_e, k_a and α are the function of frequency and amplitude of flux density. In addition, only sin-

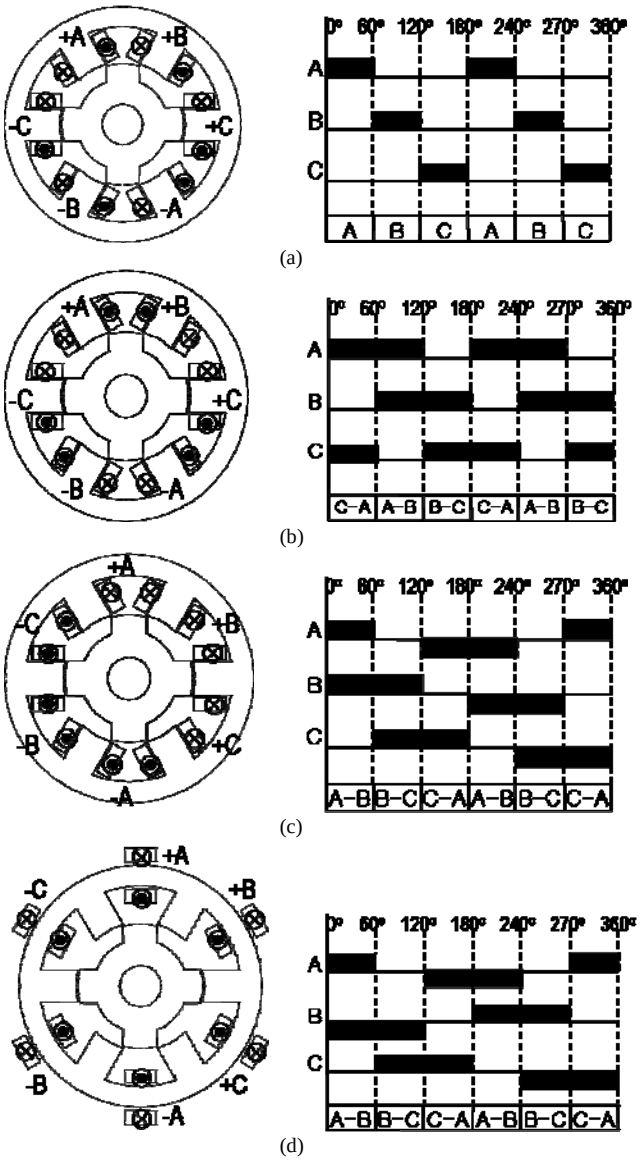

Fig. 1 The analyzed SRM models and corresponding switching sequences: (a) CSRM1; (b) CSRM2; (c) DSRM; (d) TSRM.

usoidal variable is suitable for it. The ideal exciting current of SRM has rectangular shape which will generate high harmonic flux density in the core. In this paper, a method which was proposed and verified in [7] is used to calculate the iron losses.

1) Magneto-Static Field FEA

In order to analyze the four models in the same power and ignore the extra design, the ideal exciting current source is used to generate magnetic filed. Thus, the magneto-static filed FEA is adopted in this paper. Its governing equation is expressed in (2). It can be seen that this is a typical Poisson equation.

$$\nabla \times \left[\frac{1}{\mu} (\nabla \times \boldsymbol{A}) \right] = J \tag{2}$$

where $\boldsymbol{A}$ is the magnetic vector potential, μ is the permeability, and J is the excited current density of the stator winding.

2) Harmonic Analysis

After obtain the flux density of each element, the frequency and amplitude of each harmonic component should be analyzed. In this paper, the Discrete Fourier Transform (DFT) is used. It can be expressed as

$$B_{pk}(k) = \sum_{n=0}^{N-1} B_p(n) e^{j(2\pi nk)/N} \tag{3}$$

where k is the harmonic order, N is the number of the discrete data, $B_{pk}(k)$ is the amplitude of magnetic flux density of the kth harmonic, and $B_p(n)$ is the magnitude of the point n (n=0, 1, 2,…, N-1)

When the frequencies and amplitudes of magnetic flux density at each element are obtained, depending on them, the iron losses at each element are calculated from an iron loss data sheet that is tested by the Epstein test apparatus. Then, sum the results of all harmonics and all elements, the total iron loss can be obtained. The flowchart of this calculation process is described in Fig. 2.

IV. Verification of Flux Density Variation

In FEA, each model is meshed to several thousands element. In order to represent the spatial distribution of flux density, four typical points are chosen as shown in Fig. 3. The (1) is one element in stator yoke, the (2) is one element in stator pole, the (3) is one element in rotor yoke, and the (4) is one element in rotor stator.

Fig. 4 shows the flux density variation of these four test points in the four SRM models with rotor rotation. The exciting current is 1 A in order to eliminate the saturation phenomenon. The performance of SRM can be controlled by the switch-on/off angle. In this paper, the switch-on angles of all models are 0^o rotor position.

In addition, the flux densities of these four points are decoupled into tangential and radial two parts. In the SRM,

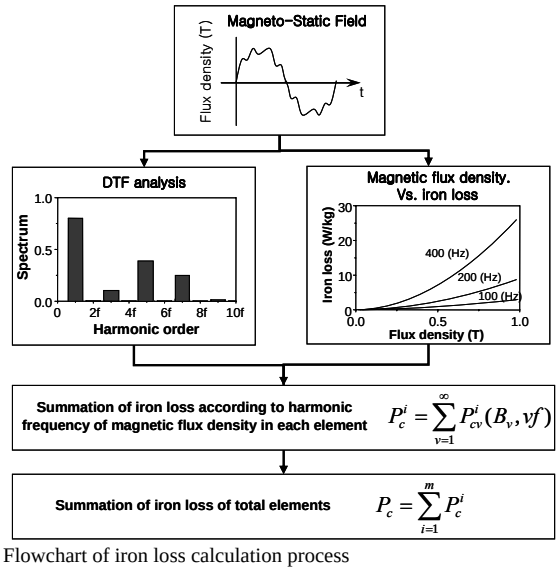

Fig. 2 Flowchart of iron loss calculation process

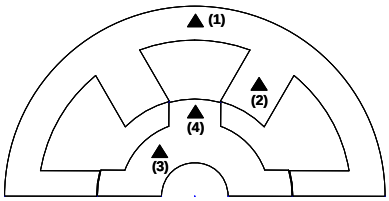

Fig. 3 Four typical elements for analysis: (1) stator yoke; (2) stator pole; (3) rotor yoke; (4) rotor pole.

TABLE II
COMPARISON OF VARIATION PERIOD IN FOUR ELEMENTS

Model	Element (1)	Element (2)	Element (3)	Element (4)
CSRM1	4	4	1	1
CSRM2	4	4	3	3
DSRM	2	2	3	3
TSRM	2	2	6	6

the magnetic filed distributes round in the stator and rotor yokes, and straight in the stator and rotor poles. Therefore, the tangential flux densities in the yokes are much greater than those in the radial direction. The adverse exists in the poles. It is also can be seen that the variation periods and amplitudes of flux densities of the same point are different, although the dimensions of these four models are completely same.

A comparison of the variation periods of flux densities is shown in Table II. The standard is the element in the rotor pole of CSRM1 whose flux density varies one period in 360 mechanical degrees.

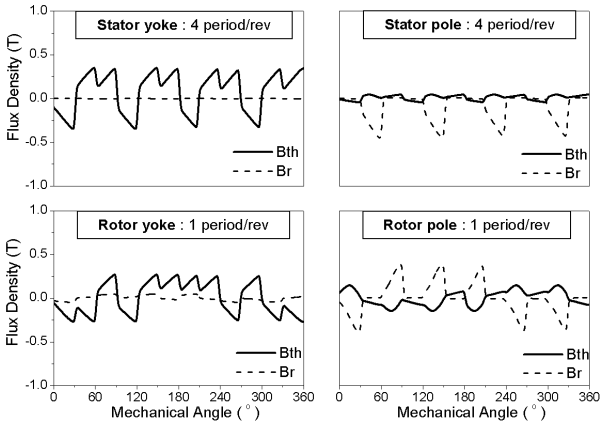

(a)

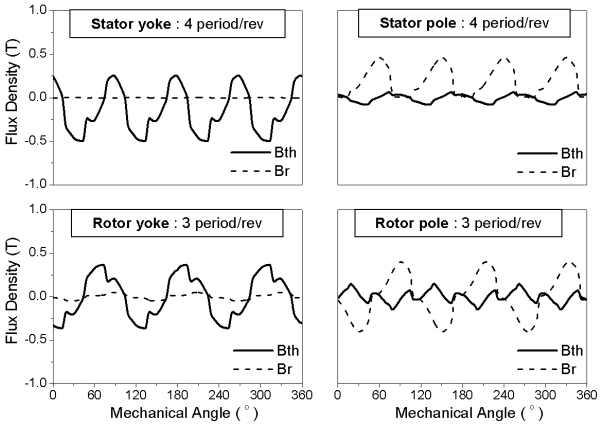

(b)

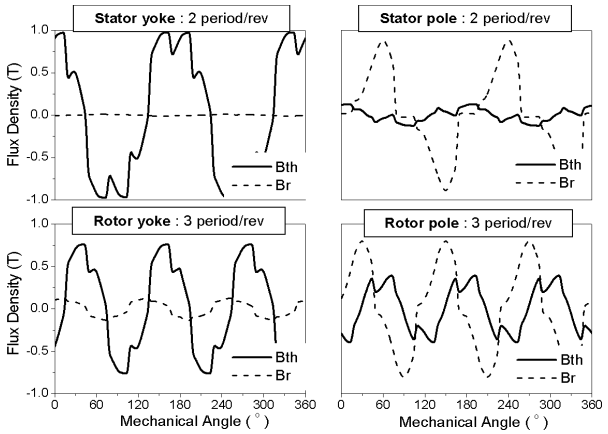

(c)

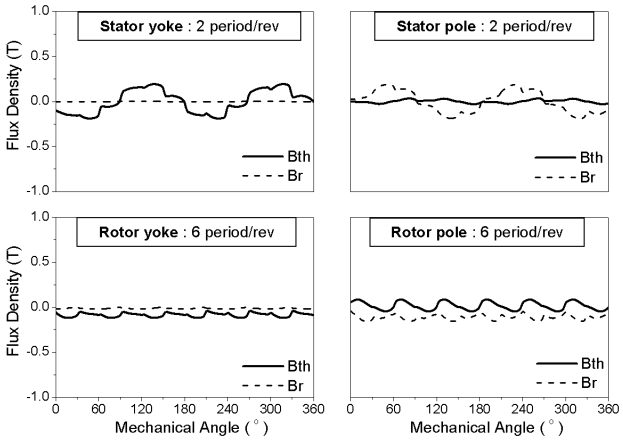

(d)

Fig. 4 Flux density variation with rotor rotation: (a) CSRM1; (b) CSRM2; (c) DSRM; (d) TSRM. (@1A excitation)

V. ANALYSIS RESULTS AND DISCUSSION

After implement DFT to the radial and tangential components of flux density of each element, the frequencies and amplitudes may be evaluated. Fig. 5 shows the total harmonic distortion (THD) of tangential components of flux densities in the element (1).

Due to the iron losses are calculated with each element, the results may be summed with any region. Fig. 6 shows the iron losses analysis results with different speed in 1 A current exciting. The iron losses in stator, rotor and total are compared individually. It is convenient to see that the iron losses of stator in CSRM1 are extremely high, while the TSRM has the lowest stator iron losses. This result is easy to be comprehended by the THD analysis. The THD of flux density in the element (1) of CSRM1 is almost three times of the one of TSRM.

In order to reveal the ratio of iron losses to input power, the transient torque of each model is evaluated and shown in Fig. 7 (a), and the average values of them are shown in Fig. 7 (b). When the rotation speed is 2000 rpm, the iron losses and ratio of iron losses to input power are compared and shown in Fig. 8 (a) and (b), respectively. The iron losses and ratio of CSRM1are chosen as the comparison references. Finally, the results as orders are summarized in Table III.

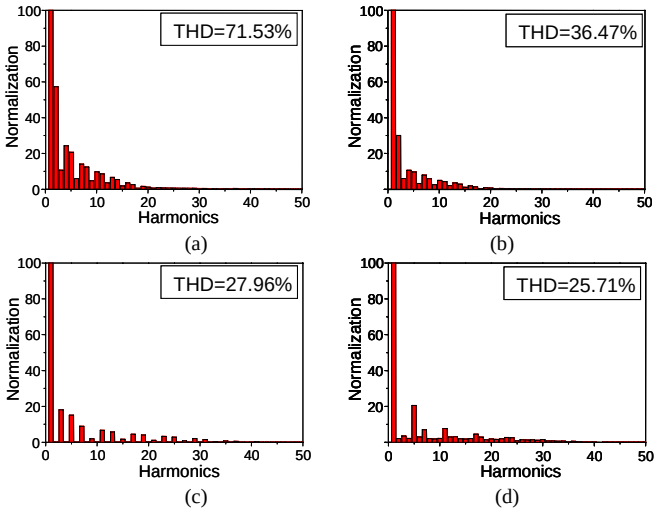

Fig. 5 THD of tangential components of flux density in element 1: (a) CSRM1; (b) CSRM2; (c) DRSM; (D) TSRM

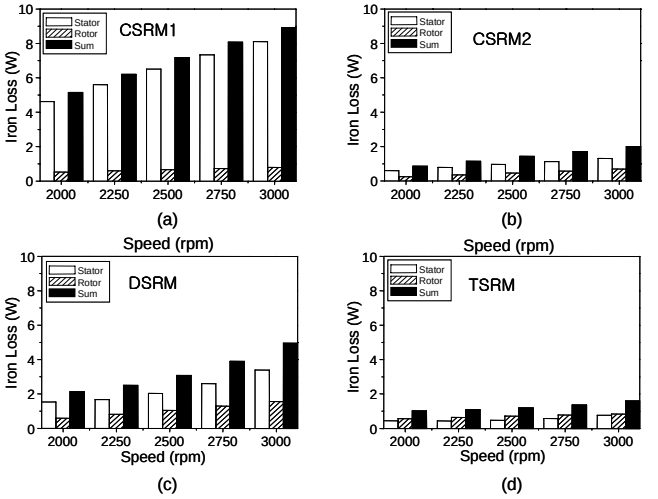

Fig. 6 Iron losses of rotor, stator and total model: (a) CSRM1; (b) CSRM2; (c) DSRM; (d) TSRM

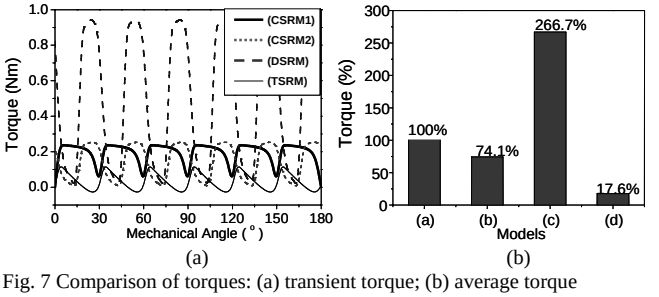

Fig. 7 Comparison of torques: (a) transient torque; (b) average torque

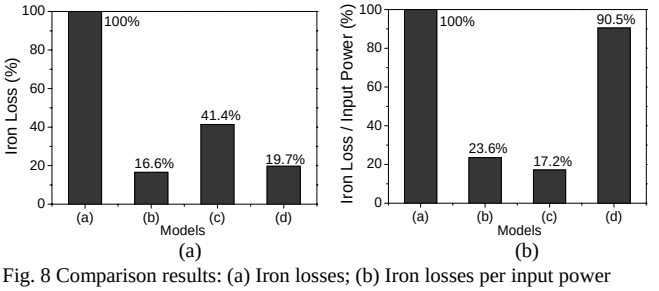

Fig. 8 Comparison results: (a) Iron losses; (b) Iron losses per input power

TABLE III
COMPARISON OF RESULTS IN ORDER

	CSRM1	CSRM2	DSRM	TSRM
THD of stator yoke	1	2	3	4
Average Torque per current	2	3	1	4
Iron losses per current	1	4	2	3
Iron losses per input power	1	3	4	2

VI. CONCLUSION

This paper deals with the iron losses evaluation and comparison in four SRM models which have different winding arrangements and/or switching sequences. The ideal rectangular current is used to be the exciting source, and hence the models with the same dimensions and number of turns can be compared. Due to the non-sinusoidal variation of the flux density, a verified numerical method which consists of magneto-static field FEA, DFT, and data curve interpolation is adopted to evaluate the iron losses of SRM. During the calculation process, the temporal variation of flux density can be observed and to give the reference to SRM design. Finally, in the analysis results, the SRM with concentrated winding and unipolar switching sequence has the highest iron losses and ratio of iron losses to input power, while the one with bipolar switching sequence has lower iron losses. Thus, for the SRM with concentrated winding, the bipolar switching sequence is suggested. Although the iron losses in DSRM is not the lowest one, the extremely high torque leads that the DSRM has the lowest ratio of iron losses to input power, i.e., for the same winding, the DSRM will get the highest efficiency. It can be seen that the SRM with bipolar switching sequence has low iron losses. This is because that the flux path is shorted in this drive method.

REFERENCES

[1] B. C. Mecrow, "New winding configurations for doubly salient reluctance machines," *IEEE Trans. Ind. Appl.*, Vol. 32, No. 6, Nov.-Dec. 1996

[2] J. W. Moon, S. G. Oh, J. W. Ahn, and Y. M. Hwang, "Drive characteristics of full-pitched winding SRM using mutual inductance," *KIEE Trans*., Vol. 47, No. 9, Sep.1998

[3] J.-W. Ahn, S.-G. Oh, J.-W. Moon, and Y.-M. Hwang, "A three phase switched reluctance motor with two-phase excitation," *IEEE Trans. Ind. Appl.*, vol. 3, no. 5, pp. 1067-1075, Sep.-Oct. 1999.

[4] J. Y. Lee, B. K. Lee, T. Sun, J. P. Hong, and W. T. Lee, "Dynamic analysis of toroidal winding switched reluctance motor driven by 6-switch converter," *IEEE Trans. Magn.*, Vol. 42. Issue. 4, pp. 1275-1278, Apr. 2006

[5] P. Rafajdus, V. Hrabovcova, and P. Hudak, "Investigation of losses and efficiency in switched reluctance motor," *EPE-PEMC.*, pp. 296-301, Aug. 2006

[6] D. M. Ionel, M. Popescu, M. I. McGilp, T. J. E. Miller, S. J. Dellinger, and R. J. Heideman, "Computation of core losses in electrical machines using improved models for laminated steel," *IEEE Trans. Ind. Appl.*, vol. 43, no. 6, pp. 1554-1564, Nov.-Dec. 2007.

[7] J. J. Lee, Y. K. Kim, H. Nam, K. H. Ha, J. P. Hong, and D. H. Hwang, "Loss Distribution of Three-Phase Induction Motor Fed by Pulsewidth-Modulated Inverter," *IEEE Trans. Magn.*, Vol. 40. No. 20, Mar. 2004